Paper # 23

Main Governing Factors Influencing Mechanical Properties of Short-cut Aramid-fibers Reinforced Elastomers

N. Vleugels, W.K. Dierkes, A. Blume, J. W. M. Noordermeer*

Dutch Polymer Institute, 5612 AB Eindhoven, the Netherlands

University of Twente, Elastomer Technology and Engineering,
7500 AE Enschede, the Netherlands

Presented at the Fall 190th Technical Meeting of
Rubber Division, ACS

October 10-13, 2016
PITTSBURG, PENNSYLVANIA
ISSN: 1547-1977

*Speaker and corresponding author j.w.m.noordermeer@utwente.nl

ABSTRACT

This study concerns short-fiber reinforcement of synthetic elastomer compounds, to gain insight into the behavior of short-cut aramid (p-phenylene terephthalamide) fibers on the processability and mechanical properties. Short-fiber reinforcement of elastomers is very complex, because it depends on many mutually interacting factors: fiber concentration, fiber orientation distribution, fiber length and distribution, fiber-matrix interfacial strength and properties of the matrix. This manuscript highlights the relationship between influencing factors in a S-SBR compound by design of experiments.

Two 3 mm long aramid fibers were chosen: one epoxy-amine-coated and one virgin fiber without coating. To potentially achieve fiber-matrix interaction the following coupling agents were selected: *Bis*-(triethoxysilylpropyl)-disulfane (TESPD), S-3-(triethoxysilylpropyl)-octanethioate (NXT), *Bis*-(triethoxysilylpropyl)-tetrasulfane (TESPT) and an alkylpolyether-mercapto-silane (Si 363). They are compared on equimolar basis with regard to the amount of reactive ethoxy-groups of TESPD. Processing of the still unvulcanized compounds and the vulcanized rubber properties are investigated.

The results show that various factor effects, and in particular the effect of fiber-matrix interaction, are grossly overshadowed by other factors: fiber concentration and orientation, respectively effects of the vulcanization system. The effect of the coupling agent is related to the interaction with adhesion active fibers, which in turn affects either the molecular integrity of the reinforced elastomer or enhances elastomer crosslinking. For each mechanical properties response an optimization prediction is calculated and confirmed with an experimental run, showing for example a 330% potential improvement in the Young's modulus.

INTRODUCTION

Research into the fundamentals of interfacial strength improvement of short-cut aramid fibers in carbon black or silica-reinforced elastomer compounds turns out to be extremely complex[1-5]. Short fiber reinforcement depends mainly on: 1) fiber concentration; 2) fiber orientation distribution; 3) fiber length and distribution; 4) fiber-matrix interfacial strength and 5) properties of the matrix[6,7]; respectively on the interdependencies between all these factors. Typical elastomer formulations contain many ingredients such as reinforcing and non-reinforcing fillers and curatives, with the fibers coming in addition, which interact either chemically or physically with each other. Many analytical tests like Fourier Transform Infrared Spectroscopy (FTIR), Differential Scanning Calorimetry (DSC) and Thermo Gravimetric Analysis (TGA) are inconclusive in elucidating these interactions. Because of the need to investigate these interactions as well as the influence of processing, a systematic study was carried out making use of a very simple/basic elastomer formulation. In particular, various publications[8-13] showed sometimes large and otherwise small improvements in mechanical properties when the interfacial strength was improved in short-cut fiber reinforced elastomer compounds. These were mainly derived from elementary tensile tests, where the effect of fibers was most conspicuous at low strains as an increase in Young's modulus and tensile strength.

The present study concerns the short-cut fiber reinforcement of synthetic elastomer compounds, with the objective to gain insight into the behavior of short-cut aramid fibers on the processability and mechanical properties. As the basis for this study a formulation was chosen, derived from the silica–reinforced passenger car tire tread technology with silane coupling agents[14], normally employed to establish chemical coupling between silica and the elastomer. The formulation was stripped to it basics by taking out the butadiene rubber, the process oil and the reinforcing filler silica or adding just a minor amount of silica, as interaction promoter between fibers and elastomer, and using the coupling agent as potential chemical binder between the fibers and the elastomer, a

solution-polymerized Styrene-Butadiene Rubber (S-SBR). 3 mm short-cut aramid fibers without finish: virgin (VF) were used of poly-p-phenylene-terephtalamide. Aramid fibers are generally very inert and consequently difficult to adhere to. The interfacial strength of the surface of an aramid fiber with a rubber can be enhanced by two main elements: an adhesive coating and an agent which can interact with this coating, a coupling agent. To make sure that interaction is established such a coating was selected, which has the ability to chemically react with a coupling agent. The coated aramid fibers selected were treated with an epoxy-amine coating[15,16] (EF), for which a typical reaction product from a model system is shown in Figure 1. The figure shows that the epoxy-groups have reacted away and are replaced by -OH hydroxyl-groups. Following this procedure, the separation of the impact of the single compound-ingredients and process conditions on properties should be possible.

DESIGN OF EXPERIMENTS

A Design of Experiments (DoE) approach was chosen, the Taguchi method[17] for a robust design. In this approach a distinction is made, with a minimal amount of experiments, between controllable factors and noise factors. The controllable factors can be manipulated directly, for example the concentration of a specific ingredient, and correspond to the factors that are normally varied in a statistical experimental design. The noise factors, for example the temperature after mixing, are resulting from the choice of the controllable factors and also have an effect on the responses, but cannot be individually influenced. Taguchi proposed that the controllable factors are varied together by means of an inner and outer array system, as shown in Figure 2. There are several ways to approach the analysis of the responses of the DoE. A common way is to use a statistical analysis of variance and perform F-tests to see which factors are statistically significant.[17] In the present manuscript a conceptual way of graphing the responses is employed, proposed by Taguchi as

an alternative, which involves visualizing the effects and identifying the factors and their interactions which appear to be significant.[18,19] The experimental data, 4 multiple data points per response per run, are analyzed by a response graph, in which the averages per experimental run (see later, Table II) and the noise averages are included. It enables the detection of scatter in responses for a particular run. So, next to the average response, it is important to register the variation in a particular response and to determine the Signal to Noise ratio (S/N), as introduced by Taguchi.[17] The S/N ratio is in its simplest form the ratio of the response average to the standard deviation. The method used to compute the ratio depends on the situation, because the S/N ratio is directly related to the choice of a particular qualifier. The qualifier 'the higher the better',[17] was chosen in the present approach, because the main interest is in the mechanical properties of the vulcanizates; even though for certain other responses, e.g. Mooney viscosity or optimum cure time, the opposite is preferred. However, the DoE allows only one qualifier throughout the whole set-up. The control factors varied in this DoE are shown in Table I. The fiber reinforced elastomer compounds contain a variety of ingredients and involve various processing steps. Therefore, in this design a selection was made of 11 factors, labelled *f*. These factors were identified on basis of a prior assessment, which seemed to have an influence on the short-cut fiber reinforcing behavior in the elastomer. The involvement of 11 factors limits the use of a statistical approach in spreadsheet form. Therefore, the conceptual way of graphing the responses was used instead. A standard experimental plan with L_{12} array of experiments was created, as shown in Table II. In this table each row corresponds to one compound and processing combination. Two types of 3 mm long fibers were chosen, see Table I, factor A. This means that the choice of a center point is not possible in the DoE, only low (level 1) and high levels (level 2). E.g., the fiber types were level 1: not coated/virgin (VF); and level 2: pre-treated with the epoxy-amine coating (EF). Four silanes were selected, representing different classes in their ability to react with the polymer and fiber-coating. The coupling agents *Bis*-(triethoxysilylpropyl)-disulfane (TESPD, Figure 3a) and *Bis*-(triethoxysilylpropyl)-tetrasulfane (TESPT, Figure 3b) belong to the

class of sulfur silanes. The coupling agents S-3-(triethoxysilylpropyl)-octanethioate (NXT, Figure 3c) and alkylpolyether-mercapto-silane (Si 363, Figure 3d) are both mercapto-silanes, the first a blocked one, the last having a free mercapto-group. All should be able to react with the hydroxyl-groups on the coated fiber surface and with the elastomer during the sulfur vulcanization. A proposed mechanism of the coating with for example the coupling agent TESPD is shown in Figure 4. The first step is the coupling reaction, where an ethoxy-silyl group of the coupling agent reacts with the coating at elevated temperature 120-140 ^{o}C. The next step is the integration of sulfur into the sulfur chain of TESPD, breaking of the sulfur bridge and finally the coupling of the sulfur radical to the elastomer. The fiber concentration was chosen as 5 and 15 parts per hundred elastomer (phr); the silica concentration at 0 and 10 phr. Silica is an inorganic filler with Si-OH groups on its surface that can form hydrogen bonds with each other and thus create filler-filler interactions to generate aggregates and agglomerates.[20-22] Generally, silica-filled compounds are improved with the help of silane coupling agents, because this creates silica-elastomer chemical bonds and so decreases the silica-silica interactions. In the present study the option of a small amount of 10 phr silica added to the compound was included in the DoE as one of the factors, to test whether it might create an additional network contribution of fiber─silane─silica─silane─fiber or fiber─silane─silica─silane─elastomer bonds. Small amounts of silica, like 10 phr are also commonly used as adhesion promoters for textile cords in elastomers.[23] Silane coupling agent concentrations used were between 0 and 1 phr for TESPD; for NXT: 0 and 1.5 phr; for TESPT: 0 and 1.1 phr; and for Si 363: 0 and 12 phr; to keep the concentration of the primary functional ethoxy-groups the same (Si-ethoxy equimolar). The curing agents concentration was varied between the standard amount[14] for silica-reinforced passenger car tread technology (level 1) and a double amount (level 2). The mixing time in the internal mixer was varied between 4 and 8 minutes, and the initial temperature setting of the mixer between 30 and 50^{o}C. The milling time after the internal mixer was varied

between 6 and 12 minutes, to ensure further fiber dispersion; the vulcanization time was varied between t_{90} and $t_{90}+2$ minutes.

With this approach the impact of variation in the chosen factors on the responses: processing performance in terms of Mooney viscosity, curing behavior and mechanical properties was investigated. Based on the optimal responses these properties can be significantly improved.

EXPERIMENTAL

MATERIALS AND COMPOUNDS PREPARATION

The formulation used in this study is given in Table III. The levels of elastomer, stearic acid and zinc oxide were not varied and represent a commonly accepted optimum level for silica-reinforced tire tread compounds.[24] Solution-polymerized styrene-butadiene elastomer (S-SBR) Buna VSL VP PBR 4045 HM from Arlanxeo, Leverkusen, Germany was used. It has styrene content of 25%wt and has 25%wt butadiene-content in the 1,2-vinyl configuration, and a Mooney viscosity $ML_w(1+4)@100^oC$ of 54 MU. Zinc oxide and stearic acid were from Sigma Aldrich, St. Louis, United States. The other ingredients which in the context of this DoE were varied are: fibers, silica, coupling agents and curing system. The two types of p-phenylene terephthalamide 3 mm short-cut fibers were provided by Teijin Aramid B.V., Arnhem, The Netherlands: Virgin Fibers without (VF) finish and an Epoxy-amine coated aramid Fiber (EF).[16] The suppliers, characteristics and structures of the coupling agents are given in Table IV and depicted in Figure 3. The sulfur was obtained from Sigma Aldrich, St. Louis, United States. The vulcanization accelerators n-Cyclohexyl-2-Benzothiazole Sulfenamide (CBS) and Diphenyl Guanidine (DPG) were provided by Flexsys, Brussels, Belgium.

The compounds were prepared based on the general mixing procedure described in Table V. The asterisk shows which factors were varied based on the descriptions in Tables I and II. A four

stages mixing procedure was used. The compounds were first mixed in a Brabender 350S internal mixer: stage I. The internal mixer chamber volume was 390 cm^3 and a fill factor of 70% was used. A fixed rotor speed was employed. In stage I, at 0 min the raw elastomer was loaded into the mixer. After 1 min the fibers, coupling agents, zinc oxide and stearic acid were added. After 3 mins the residue was swept back into the hopper. After 4 or 8 mins, factor H levels 1 or 2, the compound was discharged. The dump temperature was closely monitored in order to later link this to the coupling reaction between the silanes and the fibers[25], or some unwanted side-reactions of the coupling agent with the elastomer matrix, in particular scorch. A second masterbatch stage was employed to further disperse and homogenize the fibers on a two-roll mill during 6 or 12 mins: factor J levels 1 and 2 of the DoE. The nip-width of the mill was determined with a measuring gauge: ~30 μm. By such a thin elastomer sheet undispersed fibers could well be visually detected. After a storage time of approximately 24 hours, the second stage masterbatch was returned to the internal mixing chamber: stage 3, and mixed with the curatives up to a temperature of maximum 100°C at 75 rpm in 3 mins. The fibers in the compound were oriented in stage 4, on the mill with a nip-with of ~50 μm. With increasing mixing time the chance of fiber breakage increases. However, Hintze[8] demonstrated that this effect plays a small role for highly reinforced elastomer compounds. As the compounds employed in this study are all not reinforced with common reinforcing fillers of the carbon black and silica types, and are of the same basic formulation, it was assumed that this effect may be neglected or is at most of the same magnitude in all compounds. The obtained orientation of the fibers is shown in Figure 5, prepared with a Leica Microscope DMRX. The fibers are oriented in longitudinal direction of the milling direction.

Samples were vulcanized in a Wickert press WLP 1600 at 100 bar and 160°C to sheets of 110x110 mm, with a thickness of 2 mm, according to their t_{90} or $t_{90} + 2$ mins optimum vulcanization times, as determined with a Rubber Process Analyzer (RPA 2000) of Alpha Technologies, according to the procedure described in ISO standard 3417.

CHARACTERIZATION METHODS

The Mooney viscosity $ML_w(1+4)@100^oC$ of the compounds was measured using an Alpha Technologies Mooney 2000VS according to ISO 289. The RPA 2000 was used at 160°C to determine the curing properties: cure rate $(t_{90}\text{-}t_{s1})$ and torque increment $(M_h\text{-}M_l)$, at a frequency of 0.833 Hz and 2.79 % strain. Stress-strain measurements of all the vulcanized compounds were performed on a 3343- series Tensile Tester from Instron at crosshead speed of 500 mm/min, according to ISO 37, to determine the tensile strength at break, strain at break, Young's Modulus (YM) and Tangent Modulus (TM). The TM at 20% and 50% strain is included to emphasize the typical shape of the tensile strength vs. strain curve at low deformations below ±50% for short-cut fiber reinforced elastomers, reflected in some sort of yield strength and flattening off of the curve afterwards. The hardness of the vulcanized compounds was measured using a Zwick 3150 Shore A Hardness Tester according to ISO 7619.

CONCEPTUAL GRAPHING OF THE RESULTS OF THE DOE

In one run the mixing of each formulation was duplicated and each separate mix was tested twice on properties. Such an approach in repeating tests is needed to determine the degree of the experimental variation, designated as the replicate error. To demonstrate the benefit of the conceptual way of graphing of the responses, it is necessary to focus on measurable responses. First the processing and curing responses and later the mechanical properties are evaluated, like moduli, tensile strength at break and strain at break. As an example, the property values can first be evaluated by looking at the raw data in a replicate plot, as shown in Figure 6a. In this plot the factually measured Mooney values: $a_{k,1}$, $a_{k,2}$, $a_{k,3}$ and $a_{k,4}$, are plotted versus the number of each experimental run k. Value $a_{k,2}$ is a duplicated measurement of $a_{k,1}$ of Mix 1 and $a_{k,4}$ is a duplicated measurement of $a_{k,3}$ of Mix 2, both produced with the same control factor settings of run k. As examples runs 1 and 2

are shown in Table II. Figure 6a shows that the results per mixed compound: $a_{k,1}$ and $a_{k,2}$, resp. $a_{k,3}$ and $a_{k,4}$ are very similar and that some more variation between the duplicated mixed compounds occurs, as might have been expected. M_k is the average of all 4 measurements $a_{k,i}$ per experimental run k, see equation (1):

$$M_k = \frac{1}{4}\sum_{i=1}^{4} a_{k,i} \quad (1)$$

Since the variation in each experimental run is smaller than the spread in the averages of all runs, it can be concluded that the replicate error within a run does not complicate the overall data analysis. From here on the average M_k of the experimental run k is used to present the results.

The standard deviation s_k of the 4 $a_{k,i}$ is calculated as given in equation 2:

$$s_k = \sqrt{\frac{1}{3}\sum_{i=1}^{4}(a_{k,i} - M_k)^2} \quad (2)$$

In Figure 6a $(S/N)_k$ represents the Signal to Noise ratio 'the larger, the better', as calculated with equation 3:

$$(S/N)_k = {}^{10}\log\left(\frac{M_k}{s_k} - \frac{1}{4}\right) \quad (3)$$

The average responses M_k for Mooney viscosity level 1 resp. level 2 (Table I) for each control factor f, from A till K, are plotted in Figure 6b. To obtain an impression of the sensitivity of the mean response M_f towards the selected levels 1 or 2, a difference coefficient ΔM_f is defined for each control factor f as follows:

$$\Delta M_f = M_{f,level\,1} - M_{f,level\,2} \quad (4)$$

where $M_{f,level\,1\,or\,2}$ is the average per control factor of levels 1 or 2 for all runs k. To enlighten this calculation, see the following as an example:

$$\Delta M_A = \Delta M_{A,\,level\,1} - \Delta M_{A,\,level\,2} = (M_1+M_2+M_3+M_4+M_5+M_6)/6 - (M_7+M_8+M_9+M_{10}+M_{11}+M_{12})/6 \quad (5)$$

The difference in S/N-ratio $\Delta(S/N)$ between levels 1 and 2 for a given control factor f is shown in see Figure 6c and is calculated with equation 6:

$$\Delta(S/N)_f = (S/N)_{f,level\,1} - (S/N)_{f,level\,2} \quad (6)$$

For example:

$\Delta(S/N)_A = \Delta(S/N)_{A,\,level\,1} - \Delta(S/N)_{A,\,level\,2} = ((S/N)_1+(S/N)_2+(S/N)_3+(S/N)_4+(S/N)_5+(S/N)_6))/6 -$

$((S/N)_7+(S/N)_8+(S/N)_9+(S/N)_{10}+(S/N)_{11}+(S/N)_{12}))/6$ (7)

Figure 6d shows the ΔM_k difference coefficient and $\Delta(S/N)_k$ for Mooney viscosity, calculated with equations (4) and (6). Positive values of ΔM_f correspond to larger effects for level 1 (factors A and J) and negative values for level 2 (factors B, C, D, H and I). For example: factor B, fiber concentration, shows the largest effect to increase the Mooney Viscosity when 15 phr fiber is added (level 2), vs. 5 phr (level 1).

A grand total average over all experimental runs can be calculated with equation 8:

$$M_{total} = \frac{1}{12}\sum_{k=1}^{12} M_k \quad (8)$$

The procedure above is applied for the three DoE's (see Table I) for each factor effect. The overall results are presented in Tables VIA-D and discussed in the next section.

RESULTS AND DISCUSSION

UNDERSTANDING THE RELATIVE IMPORTANCE OF CONTROLLABLE FACTORS ON PROCESSABILITY AND MECHANICAL PROPERTIES

The Mooney Viscosity (MV) results in Table VIA of all DoE's, are represented with the qualifier 'the higher, the better', as explained before, although in general this is not always preferred in practice because of possible processing problems. The table shows the ΔM and $\Delta(S/N)$-values in percentages of the total difference including the preferred level 1 or 2 per controllable factor. The

MV difference coefficients indicate that primarily the fiber concentration (factor B, level 2) and short milling time (factor J, level 1) with a consequently lower polymer breakdown, together contribute for about 64% (DoE 1), 38% (DoE 2) and 55% (DoE 3) to a MV-increase in the DoE. The weaker contributions correspond to the use of coupling agents, e.g. factor D: 10% (DoE 1) and 22 % (DoE 3) and the application of 10 phr silica: factor C: 11% level 2 (DoE 1), 19% level 2 (DoE 2), 1% level 2 (DoE 3); the latter has a high *Δ(S/N)*- ratio, which means that this result is relatively accurate in spite of its low contribution. The effect of coupling agent Si 363, factor E in DoE 2, deviates from the other coupling agents, in the sense that it increases the Mooney viscosity, while the others tend to lower it; coupling agent NXT was neutral. Furthermore, a clear effect of 11% of the curing system is observed, even though in the present stage no vulcanization is supposed to have happened yet. The Si 363 added in its large quantities apparently gave premature scorch. As already mentioned, Si 363 is a molecule with a significantly higher molecular weight and only one ethoxy-functionality compared to the other silanes TESPT, TESPD and NXT. For this reason a much higher amount of silane was applied: a factor of appr. 10. However, this scorch effect of the Si 363 had such a large effect on all other results, that it was not further investigated or improved: the present design of experiments pointed towards an optimized formulation **without** the addition of Si 363. DoE 1 and DoE 3 also show some increase in the MV results for use of TESPD and TESPT, but no interaction with the curative system. Also for these coupling agents this most likely results from some pre-mature scorch of the elastomer, more so for TESPT than for TESPD, and more so for TESPT, because the former contains more elemental ts molecule. But by far not as much as for Si 363. NXT shows no pre-mature scorch and coupling could only occur with the coating. Furthermore, TESPD and TESPD have two $Si(OEt)_3$-groups on each side, which might create some silane-bridges in addition, which NXT cannot do because of its single $Si(OEt)_3$-group. Unfortunally, the MV data seem not sensitive

enough to separate/detect coupling to the fibers from the scorch effect; the DoE is not able to resolve this question: this scorch is a typical noise factor.

The Mooney viscosity tends to increase by the use of VF vs. the coated EF in DoE 1, an effect which could possibly be related to the coating itself[26], though the results from DoE 2 and 3 show no clear trend.

Table VIB shows the results for vulcanization behavior of the compounds. The use of more fibers (15 vs. 5 phr) and more curatives (double vs. single dosage) generally result in higher M_h-M_l. Together they contribute for DoE 1 64%, for DoE 2 50% and DoE 3 57%. The (M_h-M_l)-data show some dependency on factor H, Internal Mixer Mixing Time: for DoE 1 16%, DoE 2 12% and DoE 3 14%. In each design the shorter mixing time (level 1) is favored, which we relate to less polymer breakdown during shorter mixing, another noise factor in the context of the DoE's. The coupling agent factors D and E seem to play only a small role. Coupling agent Si 363 tends to level 1 for the ΔM: preferentially no coupling agent added, which again points at the disturbing effect of Si 363 as a disturbing factor in the curing due to its premature scorch during mixing: much more than the other coupling agents.

The vulcanization speed t_{90}-t_{s1} is in all DoE designs not influenced by the fiber concentration, as might have been expected beforehand, but only by the coupling agent's factors D and E and curatives concentration factor G. Most surprising is that factor H, internal mixer time, again plays an important role for t_{90}-t_{s1}, for DoE 1 19%, for DoE 2 13% and for DoE 3 8%. This effect indicates that the dispersion of the curatives is improved by a longer mixing time or that this again is related to the polymer breakdown noise effect. Also factor I, the initial mixer temperature setting, has a clear effect on the results, again an indication polymer breakdown effects. The way of processing the compounds apparently plays a major role in the vulcanization properties. This effect may not be underestimated in the judgement of fiber-matrix interaction

The effects of short fibers are most clearly seen in the tensile properties at low strains.[27] The short fibers commonly raise the Young's modulus and create a yield point at typically low strains. After the yield point, the interaction between fibers and elastomer becomes too weak and the tensile curve follows the non fiber-reinforced elastomer path. In the present study none of compounds reaches a clear yield point, because they fail before that strain. The results for the moduli: the Young's modulus and the Tangent Moduli at 20 and 50% strain ($TM_{20\%}$ and $TM_{50\%}$) are given in Table VIc. Because the results of the DoE's for the Young's modulus are most eye-catching, the Difference Coefficients for the Young's modulus for DoE1 are represented as an example of the conceptual way of graphing the responses against the control factors *f* in Figure 7. The Young's modulus most strongly rises for all three DoE's for factor B level 2: increased fiber concentration, compared to all other factors. Factor C level 2, the addition of 10 phr silica, tends to decrease the Young's modulus, but increases the strength and strain at break: see Table VId. It is an indication that the concentration of 10 phr silica is still below the percolation threshold, where silica starts to act as a common reinforcing filler. As it turns out, the addition of silica increases the strain at break substantially due to the discussed coupling reaction in interaction with the coupling agents, as discussed before. This is also confirmed by the difference coefficient in the $TM_{20\%}$ and $TM_{50\%}$ data, already taken at higher strain compared to the Young's modulus. The calculation for $TM_{50\%}$ for DoE1 could not be made, as run 12 did not reach 50% strain at break and because results of all runs are required for a proper analysis. This indicates indeed that before 50% strain the main effects of fiber reinforcement are seen, as stated before. Overall, the effects of the coupling agents are still comparatively weak compared to other factors, like fiber concentration, fiber orientation and silica usage. The *YM* and $TM_{20\%}$ difference coefficients for factor J, milling time, seem to be favored by a longer duration of milling: level 2; for $TM_{50\%}$ in DoE 3 the tensile curve has practically levelled off so that the preference is for the opposite level 1. Consequently, the better tensile properties are clearly related to a better dispersion of the fibers. This makes it unlikely at the same time that fiber

breakage has a significant negative effect on the results. The internal mixer mixing time factor has a strong effect on the moduli, generally pointing to level 1, short mixing time as preferred: again most probably related to less polymer breakdown. As explained before, this is caused by less polymer breakdown: the noise effect. However, the corresponding $\Delta(S/N)$'s of factor H are rather low, especially for the $TM_{50\%}$, therefore minimize the importance of this effect.

A yield point in the tensile properties was practically not observed for none of the compounds, apparently because they had a too low intrinsic strength by absence of carbon black or silica reinforcement. Therefore, a yield point could not be used as a response in terms of the DoE's. The DoE results for tensile strength at break and strain at break as represented in Table VID are therefore not very conclusive. They show that the strength at break is primarily increased by fiber concentration and to a lesser extent by the amount of curatives added. In DoE 2, coupling agent Si 363 clearly decreases the strength at break, again as a result of its premature scorch and consequently poor vulcanization. The addition of 10 phr silica: factor C level 2; adding coupling agents TESPD and Si 363, level 2; long milling time, factor J level 2, all increase the strain at break. This combination points to a beneficial effect of the use of some silica in combination with the CA TESPD, as might have been expected on basis of the use of silica as reinforcing filler together with coupling agents in passenger tire technology.[14]

The effects of orientation were not very clear, as they were greatly overruled by the other factors. It was noticed that the low 5 phr fiber containing compounds behaved fundamentally different from the ones with 15 phr, as far as their response on orientation was concerned. Surprisingly, in a separate series of experiments (not mentioned here) a low dosage of non-oriented fibers gave the highest YM vs. longitudinally or transversely oriented fibers, irrespective of whether they were EF or VF. For 15 phr fibers, longitudinally oriented fibers gave clearly the highest contribution. Apparently, the factual mechanical mechanism of the reinforcement effect of short-cut

fibers interchanges in between 5 and 15 phr: another noise factor no covered by the present DoE's. This will be reported in a later manuscript.

Overall, the EF in combination with the various coupling agents, except for Si 63, gives the higher *YM's*, as an indication for fiber-elastomer interaction. A mutual comparison of the effects of the different coupling agents cannot be made yet at this point but needs the confirmation runs to finalize the DoE approach.

OPTIMAL MECHANICAL PROPERTIES

Each DoE is completed with a conformation run. A prediction of the possible improvement for a particular response can be made with the following equation:

$$\mu = M_{total} + \sum_{f=1}^{11} (M_{f,optimum\ level\ 1\ or\ 2} - M_{total}) \tag{9}$$

where μ is the overall optimized response and $M_{f,optimum\ level\ 1\ or\ 2}$ is the best level (highest average value) of the two M_f levels 1 or 2 of each factor. In Tables VIA-D these results are summarized. The tables show the optimal μ obtainable for each given response, by selecting the best level of each controllable factor. The optimization results show very large improvements in comparison with the average M_{total} values. To experimentally validate the calculated results per DoE, an optimization run was performed for a maximum Young's modulus: the optimized tensile test curve presented in Figure 8 for DoE1 making use of EF and NXT coupling agent; in Figure 9 for DoE3 making use of EF and TESPD, and with TESPT from DoE2 included to visualize the difference between the two latter coupling agnets, based on the highest mean effect results for *YM*. The M_{total} is added for comparison. An improvement is found for DoE's 1-3 of 233-330% for the YM, where coupling agent NXT in combination with EF gives the highest reinforcement in *YM* as shown in Figure 8. This demonstrates that the present DoE-approach indeed enables to identify the most important properties

and to find the optimum compound composition and processing conditions, despite the sometimes large differences in $\Delta(S/N)$ ratios, in this enormously complicated field of mutually interacting factors.

A limitation of the DoE used in this study is its sensitivity towards the optimum reaction temperature for the CA's. The mixing discharge temperatures of the experimental runs differ between 120°C and 140°C. A reaction temperature study needs to be executed in a follow-up series of experiments to identify the optimum coupling temperature for each coupling agent. As they may differ amongst each other.

CONCLUSIONS

This study concerns the understanding of the relative importance of controllable factors on the processability and mechanical properties, resp. the optimization of the performance of short-cut fiber reinforced elastomers with the help of a Design of Experiments (DoE) approach. A Taguchi conceptual way of graphing approach in the design of experiments is a valuable tool to investigate the relative importance of such controllable factors on the processability and mechanical properties of short-cut fiber reinforced elastomers. Every factor is compared on basis of equal footing, which highlights the relative importance of each factors response. The experimental objective was to determine the impact of both compounding ingredients and processing parameters on the Mooney viscosity, the vulcanization performance and mechanical properties of the resulting vulcanizates.

The results clearly show that some factor effects are fully or partially overshadowed by other factors: fiber concentration and curatives concentration grossly overrule all other factors in their effect on the Young's modulus, the latter being most representative for the mechanical properties. Interaction between fibers and elastomer plays only a secondary role, whereby the epoxy-amine coated fibers in combination with coupling agent NXT gave overall the best results. To increase the

effect of the factors which are now overshadowed, the difference between levels 1 and 2 needs to be increased. To for example investigate the effect of silane coupling agents, factor E (NXT content in DoE 1) needs to be varied over a wider range, while the other factors are kept constant. To obtain a large increase in mechanical properties, in particular at low strains: Young's modulus, the fiber concentration needs to be increased rather than the curing time. For each mechanical property response an optimization prediction was calculated on basis of the mean values of all runs, varying between 126 and 300% improvement. A confirmation run confirmed this optimization for the Young's modulus. The effect on the YM can be increased with 233-330%, just by choosing the higher level value in the DoE factor settings. The eventual mechanical properties reached in the conformation run are comparable to the predicted results μ, confirming the value of the DoE approach. This method is also suitable to visualize smaller effects, just by focusing on one factor by a time and changing the levels, how this will influence μ.

ACKNOWLEDGEMENTS

The authors are indebted to Dutch polymer Institute (DPI) for financial support of this work and permission to publish this work under project #782. Mrs. J. Jansen† and Dr. L.A.E.M. Reuvekamp of Apollo Vredestein Global R&D are gratefully acknowledged for assistance with the Design of Experiments set-up.

REFERENCES

[1] S. Abrate, RUBBER CHEM. TECHNOL, **59**(3), 384-404 (1986).

[2] J. Kalantar and Drzal L.T., *J. Mat. Sci.*, **25**(10), 4186-4193 (1990).

[3] M.A. López Manchado and Arroyo M., *Polym. Comp.*, **23**(4), 666-673 (2002).

[4] C. Hintze, R. Stoček, T. Horst, R. Jurk, S. Wießner and G. Heinrich, *Pol. Eng. Sci.*, **54**(12), 2958-2964 (2014).

[5] C. Hintze, R. Boldt, Wießner, S. and Heinrich, G., *Kautsch. Gummi Kunstst*., **67**(9), 42-46 (2014).

[6] S. Fu, B. Lauke and Y Mai, *Science and engineering of short fiber reinforced polymer composites*, Woodhead Publishing, Cambridge, England (2009).

[7] S. K. De and J. R. White, *Short fibre polymer composites*, Woodhead Publishing, Cambridge, England (1996).

[8] J. E. O'Connor, RUBBER CHEM. TECHNOL., **50**(5), 945 958 (1977).

[9] A. Y. Coran, K. Boustany, and P. Hamed, *J. Appl. Pol. Sci.*, **15**(10), 2471-2485 (1971).

[10] Y. B. Aziz, *Composites of natural elastomer and polyaramid short fibres*, Loughborough University, PhD-thesis (1981).

[11] G.S. Shibulal and K. Naskar, *Polym. Comp.*, **35(9)**, 1767-1778, (2013).

[12] C. Hintze, *Influence of processing induced morphology on mechanical properties of short aramid fibre filled elastomer composites*, University of Dresden, Germany, PhD-Thesis (2012).

[13] M. Shirazi, *Aromatic polyamide short fibres reinforced elastomers*, University of Twente, Enschede, the Netherlands, PhD-Thesis (2013).

[14] R. Rauline (to Compagnie Generale des Establissements Michelin) EU 0501227 (1992).

[15] J. Mahy et al., in *Van Ooij W J, Anderson Jr H R, eds., Mittal Festschrift*, 1st International Congress on Adhesion Science and Technology, VSPI, Utrecht, the Netherlands, pgs. 407-425 (1998).

[16] P. de Lange, *Compos. Part A: Appl. Sci. Manuf.*, **32,** 331-342 (2001).

[17] D. M. Byrne and S. Taguchi, *American Society for Quality Control. Inc.* Milwaukee, Wisc. USA, (1987).

[18] L. Eriksson et al. *Design of experiments*, 3th revision, Umetrics Academy, Umeå, Sweden (2008).

[19] R. J. Del Vecchio, *Understanding Design of Experiments*, Hanser/Gardner Inc., Cincinnati, USA (1977).

[20] M.J. Wang, , RUBBER CHEM. TECHNOL, **71**(3), 520-589 (1998).

[21] A. Blume, *Kautsch. Gummi Kunstst*., **53**(6) 338-345 (2000).

[22] L. A. E. M Reuvekamp, *Kautsch. Gummi Kunstst.*, **62**(1-2) 35-43 (2009).

[23] J. D. Minford, *Treatise on adhesion and Adhesives*, CRC Press, New York, U.S.A., **7**, 261-262 (1990).

[24] L. Guy, S. Daudey, P. Cochet and Y. Bomal, *Kautsch. Gummi Kunstst*, **62,** 383-391 (2009).

[25] W. K. Dierkes, *Kautsch. Gummi Kunstst*. **60**, 614-618 (2007)**.**

[26] P. Lange, Teijin Aramid BV, private communication.

[27] M. Shirazi and J.W.M. Noordermeer, RUBBER CHEM. TECHNOL., **84**(2), 187-199 (2011).

TABLE I

TAGUCHI DESIGN: VARIED CONTROL FACTORS

		DOE 1, 2, 3	DOE 1	DOE 2	DOE 3
Factor f		Level 1	Level 2	Level 2	Level 2
A	Fiber type:	Not coated (VF)	Coated (EF)	→	→
B	Fiber conc.:	5 phr	15 phr	→	→
C	Filler:	0	10 phr silica	→	→
D	Coupling with*:	0	1 phr TESPD	1.1 phr TESPT	1.1 phr TESPT
E	Coupling with*:	0	1.5 phr NXT	12 phr Si 363	1 phr TESPD
F	Orientation**:	0^o	90^o	→	→
G	Curatives conc.:	single	double	→	→
				→	→
H	Internal mixer mixing time:	4 (mins)	8 (mins)	→	→
I	Internal mixer T_{in}:	30 (^{o}C)	50 (^{o}C)	→	→
J	Mill mixing time in stage 2:	6 (mins)	12 (mins)	→	→
				→	→
K	Curing time:	t_{90} (mins)	t_{90} + 2 (mins)	→	→

*Corresponds to equal amounts of ethoxy-functional groups to TESPD

**0^o Longitudinal orientation and 90^o transverse rel. to milling direction

TABLE II

SHORT FIBER REINFORCED COMPOUND TAGUCHI BASED EXPERIMENTAL PLAN

Runs	Control factors f											Compound 1		Compound 2				
k	A	B	C	D	E	F	G	H	I	J	K	$a_{k,i}$				M_k	s_k	$(S/N)_k$
1	1	1	1	1	1	1	1	1	1	1	1	$a_{1,1}$	$a_{1,2}$	$a_{1,3}$	$a_{1,4}$	M_1	s_1	$(S/N)_1$
2	1	1	1	1	1	2	2	2	2	2	2	$a_{2,1}$	$a_{2,2}$	$a_{2,3}$	$a_{2,4}$	M_2	s_2	$(S/N)_2$
3	1	1	2	2	2	1	1	1	2	2	2	Etc.				Etc.		
4	1	2	1	2	2	1	2	2	1	1	2							
5	1	2	2	1	2	2	1	2	1	2	1							
6	1	2	2	2	1	2	2	1	2	1	1							
7	2	1	2	2	1	1	2	2	1	2	1							
8	2	1	2	1	2	2	2	1	1	1	2							
9	2	1	1	2	2	2	1	2	2	1	1							
10	2	2	2	1	1	1	1	2	2	1	2							
11	2	2	1	2	1	2	1	1	1	2	2							
12	2	2	1	1	2	1	2	1	2	2	1							
																M_{total}		

*The numbers 1 and 2 refer to level 1 and level 2.

TABLE III

STANDARD ELASTOMERIC COMPOUND FORMULATION

Formulation	(phr)
S-SBR	100
Coupling agent, based on TESPD	1*
Silica	0 or 10*
Zinc oxide	2.5
Stearic acid	1.5
Short fiber	5 or 15* VF/EF
Sulfur	1.4 or 2.8*
CBS[e]	1.7 or 3.4*
DPG[f]	2.0 or 4.0*

*varied depending on experimental plan, see Tables I and II

[e]N-Cyclohexyl-2-benzothiazole sulfenamide

[f]Diphenyl Guanidine

TABLE IV

CHARACTERISTICS OF COUPLING AGENTS USED IN THIS RESEARCH

Silane coupling agent	Chemical formula	Cas nr.	MW, g/mol	Density, g/cm^3
TESPD[a]	$C_{18}H_{42}O_6S_2Si_2$	56706-10-6	475	1.03
NXT[b]	$C_{17}H_{36}O_4SSi$	220727-26-4	365	0.97
TESPT[a]	$C_{18}H_{42}O_6S_4Si_2$	254-896-5	539	1.08
Si 363[a]	$C_{55}H_{114}O_{15}SSi$	69011-36-5	1075	1.01

[a] Si 75, Si 69, Si 363 Evonik Industries AG, Essen, Germany

[b] NXT*silane Momentive GE Silicones, Wilton, CT, United states

TABLE V

FOUR STAGES MIXING PROCEDURE

1st masterbatch stage: Brabender 350 S		
Rotor speed	110	rpm
Initial temperature setting*	30/50	°C
Fill factor	70	%
Steps in mins:	0	Add polymer
	1	Add 50% fiber, silane*
	1.5	Add 50% fiber
	2	Silica*, zinc oxide, stearic acid
	3	Sweep
	4	Dump @ ~ 120-140 °C
2nd masterbatch stage – remix: Two-roll mill		
Add to mill to further disperse fibers		
Friction ratio	1:1.3	
Nip width	~0.03	mm
Steps in mins:	6 min or 12 min *	
3rd masterbatch stage: Brabender 350 S		
Rotor speed	75	rpm
Initial temperature setting	50	°C
Fill factor	70	%
Steps in mins:	0	Add batch from stage 2
	1	Add curatives
	3	Dump @ ~ 100 °C
4th masterbatch stage: Two-roll mill		
Orient fibers on the mill and make sheet		
Time	~2	mins
	~0.05	mm

*varied depending on experimental plan, see Tables I and II.

TABLE VIA

MOONEY VISCOSITY RESPONSES FOR GIVEN CONTROL FACTORS

		DoE 1				DoE 2				DoE 3			
		ΔM		*ΔS/N*		*ΔM*		*ΔS/N*		*ΔM*		*ΔS/N*	
Factor effects		L	%	L	%	L	%	L	%	L	%	L	%
A	Fiber type:	1	10	2	4	1	1	1	18	2	3	1	14
B	Fiber conc.:	2	38	2	22	2	28	2	3	2	31	1	2
C	Filler:	2	11	1	1	2	19	1	12	2	1	2	17
D	CA A:	2	10	2	16	1	3	1	1	2	22	2	13
E	CA B:	1	0	1	16	2	6	1	18	2	5	2	23
F	Orientation:	-	-	-	-	-	-	-	-	-	-	-	-
G	Curatives conc.:	1	0	1	5	1	11	2	22	1	0	1	15
H	Internal mixer mix. time:	2	2	2	5	2	10	1	1	2	3	2	6
I	T_{in}:	2	2	1	11	2	11	2	16	2	12	2	8
J	Mill mix. Time	1	26	2	20	1	10	1	9	1	24	2	12
K	Curing time:	-	-	-	-	-	-	-	-	-	-	-	-
M_{total}		41				65				47			
μ		62				137				75			
$(\mu \cdot 100)/ M_{total}$ (%)		151				211				160			

L = 1: preference for level 1; 2: preference for level 2; -: no preference.

TABLE VIB

M_H-M_L AND T_{90}-T_{S1} RESPONSES FOR GIVEN CONTROL FACTORS

		M_h-M_l										t_{90}-t_{s1}									
		DoE 1				DoE 2				DoE 3				DoE 1				DoE 2				DoE 3			
		ΔM		*ΔS/N*		*ΔM*		*ΔS/N*		*ΔM*		*ΔS/N*		*ΔM*		*ΔS/N*		*ΔM*		*ΔS/N*		*ΔM*		*ΔS/N*	
	Factor effects f	L	%	L	%	L	%	L	%	L	%	L	%	L	%	L	%	L	%	L	%	L	%	L	%
A	Fiber type:	2	7	2	5	2	4	2	4	2	5	1	6	2	4	2	8	1	0	1	3	2	9	2	15
B	Fiber conc.:	2	27	2	13	2	22	1	35	2	21	1	9	2	4	1	3	1	5	1	4	2	3	2	26
C	Filler:	1	2	2	1	2	6	2	8	2	6	2	13	1	8	2	14	1	3	2	1	1	3	1	3
D	CA A:	1	2	2	13	2	12	2	5	2	4	2	11	2	23	1	26	2	17	2	12	1	13	1	1
E	CA B:	2	3	1	10	1	4	1	6	1	11	2	22	2	11	1	18	2	26	1	29	1	23	1	10
F	Orientation:	-	-	-	-	-	-	-	-	-	-	-	-	-	-	-	-	-	-	-	-	-	-	-	-
G	Curatives conc.:	2	37	1	10	2	28	2	14	2	36	1	5	1	28	2	5	1	25	1	2	2	28	2	6
H	Internal mixer mix. time:	1	16	2	1	1	12	1	8	1	11	2	6	2	19	2	6	2	13	1	21	2	8	2	2
I	T_{in}:	2	5	1	33	1	7	1	16	2	4	1	13	2	4	1	7	2	10	2	3	1	0	1	14
J	Mill mix. Time	2	2	2	14	1	5	2	6	1	3	2	14	0	0	1	13	1	1	2	24	1	13	1	23
K	Curing time:	-	-	-	-	-	-	-	-	-	-	-	-	-	-	-	-	-	-	-	-	-	-	-	-
M_{total}		6				5				6				4				6				5			
μ		10				9				9				11				18				12			
(μ 100)/ M_{total} (%)		170				180				170				240				300				220			

TABLE VIc

RESPONSES FOR GIVEN CONTROL FACTORS: YOUNG'S MODULUS AND TANGENT MODULUS AT 20 AND 50% STRAIN

		Young's modulus											
		DoE 1				DoE 2				DoE 3			
		ΔM		*ΔS/N*		*ΔM*		*ΔS/N*		*ΔM*		*ΔS/N*	
Factor effects f		L	%	L	%	L	%	L	%	L	%	L	%
A	Fiber type:	2	12	2	9	2	3	2	18	2	15	2	6
B	Fiber conc.:	2	29	2	2	2	23	1	16	2	24	2	6
C	Filler:	1	10	1	9	1	2	2	5	1	6	1	6
D	CA A:	1	0	1	17	2	14	2	20	1	5	2	8
E	CA B:	2	2	2	1	1	24	1	3	2	9	2	3
F	Orientation:	1	2	1	4	2	8	2	5	1	10	1	11
G	Curatives conc.:	2	9	2	3	2	2	2	10	2	8	1	7
H	Internal mixer mix. time:	1	17	1	9	1	14	2	2	1	8	1	11
I	T_{in}:	2	8	2	17	1	6	1	12	2	9	2	18
J	Mill mix. Time	2	6	2	23	2	3	1	0	2	5	2	23
K	Curing time:	1	5	2	6	1	1	1	10	1	3	1	0
M_{total}		9				3				5			
μ		29				7				20			
$(\mu\ 100)/\ M_{total}$ (%)		332				233				380			

	Tangent Modulus 20% strain												*Tangent Modulus 50% strain*							
	DoE 1				DoE 2				DoE 3				DoE 1	DoE 2				DoE 3		
	ΔM		*ΔS/N*		*ΔM*		*ΔS/N*		*ΔM*		*ΔS/N*			*ΔM*		*ΔS/N*		*ΔM*		*ΔS/N*	
	L	%	L	%	L	%	L	%	L	%	L	%		L	%	L	%	L	%	L	%
A	2	14	2	2	2	2	1	3	2	14	1	1		2	3	2	5	2	17	2	6
B	2	30	1	1	2	24	1	8	2	25	2	4		2	25	1	2	2	32	2	8
C	1	11	1	12	1	0	1	1	1	5	1	9		1	1	2	1	1	2	1	9
D	0	0	1	18	2	14	2	16	1	7	2	2		2	11	2	12	2	5	2	5
E	2	2	1	5	1	26	2	10	2	4	2	14		1	26	1	9	2	9	2	10
F	1	3	2	10	2	10	1	14	1	11	1	11	*n/a*	2	1	1	17	1	9	1	10
G	2	8	2	4	2	2	2	21	2	7	2	2		2	6	2	14	2	4	2	14
H	1	16	1	5	1	14	2	4	1	10	1	7		1	13	1	2	1	2	0	0
I	2	6	2	17	1	5	2	2	2	8	2	17		1	5	1	14	2	5	2	5
J	2	6	2	21	2	2	1	5	2	3	2	28		2	3	2	7	1	5	2	27
K	1	3	2	5	1	1	1	17	1	5	1	5		1	6	1	17	2	9	1	5
	7				3				5					2				4			
	22				7				17					5				7			
	305				260				350					230				180			

TABLE VIᴅ

RESPONSES FOR GIVEN CONTROL FACTORS: STRESS AND STRAIN AT BREAK

		Stress at break										*Strain at break*									
		DoE 1				DoE 2				DoE 3				DoE 1				DoE 2				DoE 3			
		ΔM		*ΔS/N*		*ΔM*		*ΔS/N*		*ΔM*		*ΔS/N*		*ΔM*		*ΔS/N*		*ΔM*		*ΔS/N*		*ΔM*		*ΔS/N*	
	Factor effects	L	%	L	%	L	%	L	%	L	%	L	%	L	%	L	%	L	%	L	%	L	%	L	%
A	Fiber type:	2	10	2	8	2	5	2	11	2	13	2	2	1	15	2	13	1	2	2	25	1	13	1	4
B	Fiber conc.:	2	39	1	14	2	15	2	0	2	21	1	7	1	14	2	1	1	31	1	14	1	14	1	14
C	Filler:	2	7	2	13	2	16	2	10	2	9	2	13	2	20	1	10	2	20	2	10	2	18	1	1
D	CA A:	2	5	2	5	2	11	2	1	2	3	2	20	2	9	1	9	2	0	1	0	2	1	2	18
E	CA B:	1	2	1	11	1	23	1	25	2	12	2	11	0	0	1	0	2	18	2	13	2	14	2	11
F	Orientation:	1	7	1	12	0	0	2	6	1	10	1	16	0	1	2	7	2	1	2	2	2	2	2	2
G	Curatives conc.:	2	13	1	3	2	7	2	5	2	13	2	6	1	16	2	17	1	15	1	2	1	16	2	1
H	Internal mixer mix. time:	1	11	2	14	1	6	2	29	1	5	2	1	2	4	1	0	2	4	2	11	2	3	2	10
I	T_{in}:	2	4	2	9	1	3	2	1	2	5	2	6	1	6	2	11	2	5	2	11	1	2	2	11
J	Mill mix. Time	0	1	2	3	2	8	2	9	2	7	2	13	2	12	2	31	2	2	1	2	2	11	2	18
K	Curing time:	2	2	1	8	1	5	1	2	1	2	1	5	1	3	1	1	1	2	2	9	1	5	2	10
M_{total}		5				3				5				210				240				230			
μ		8				9				10				640				450				650			
$(\mu \cdot 100)/ M_{total}$ (%)		160				300				210				310				190				280			

CAPTIONS TO THE FIGURES

Figure 1: Schematic representation of the reaction product observed in the epoxy-based finish model system.

Figure 2: Part of the experimental design with low and high levels, without central point.

Figure 3: Silane coupling agents a) TESPD, b) TESPT, c) NXT and d) Si 363.

Figure 4: Proposed reaction mechanism of TESPD with epoxy coated fiber and elastomer.

Figure 5: Orientation of the fibers, visualized with a Leica microscope DMRX.

Figure 6: a) Raw data replicate plot of Mooney viscosity (MU), b) Mean Mooney viscosity per level per factor, c) *S/N* ratio's *MV* per level per factor and d) Difference coefficients for *MV* (MU) per factor.

Figure 7: Conceptual way of graphing the Difference coefficients for Young's modulus (MPa) per control factor for DoE1.

Figure 8: Tensile curve optimized for *YM* vs. M_{total} values for DoE1.

Figure 9: Tensile curve optimized for *YM* vs. M_{total} values for DoE's 2 and 3.

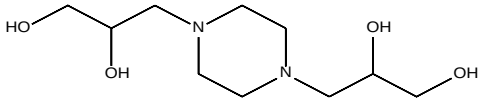

3,3'-(piperazine-1,4-diyl)bis(propane-1,2-diol)

FIG. 1 ─ Schematic representation of the reaction product observed in the epoxy-based finish model system.

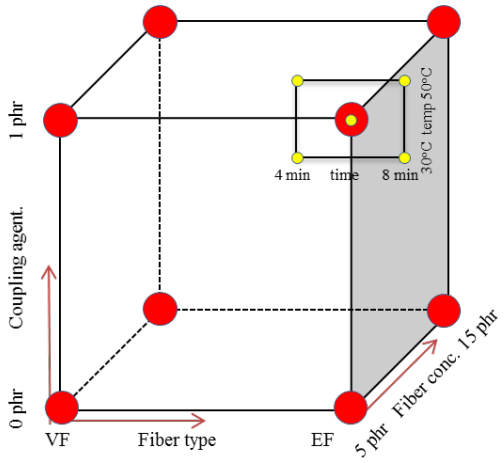

FIG. 2. — Part of the experimental design with low and high levels, without central point.

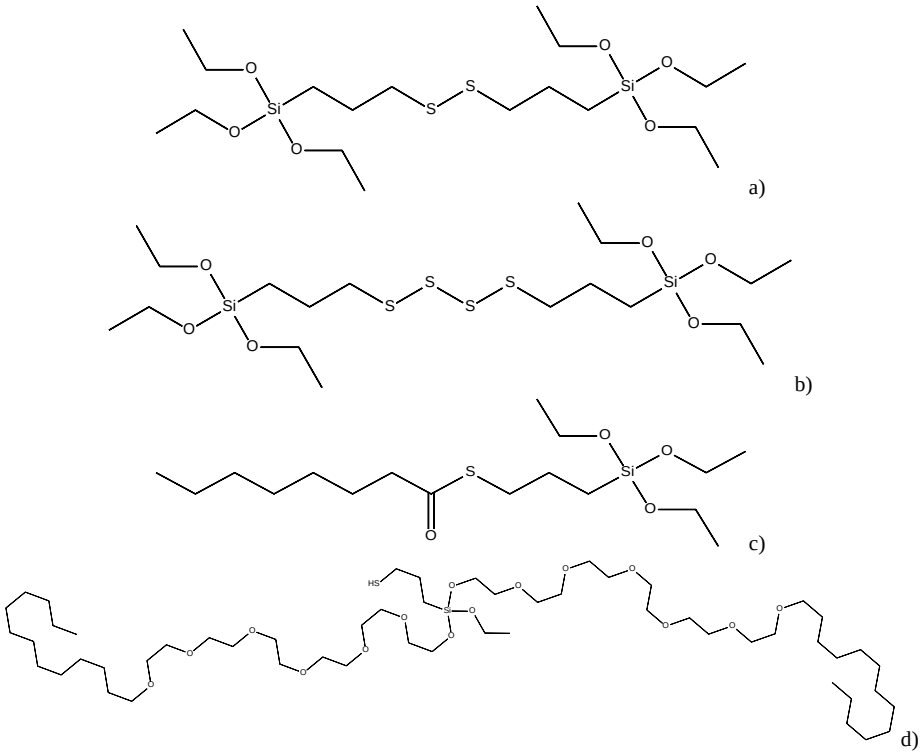

FIG. 3 ─ Silane coupling agents a) TESPD, b) TESPT, c) NXT and d) Si 363.

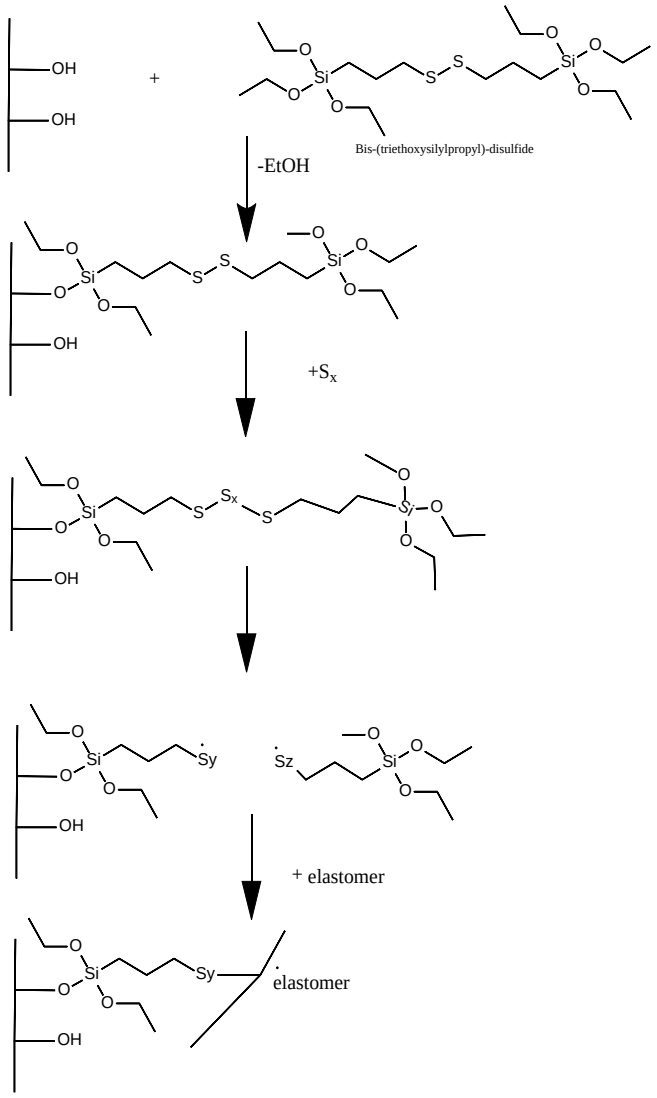

FIG. 4 ─ Proposed reaction mechanism of TESPD with epoxy coated fiber and elastomer.

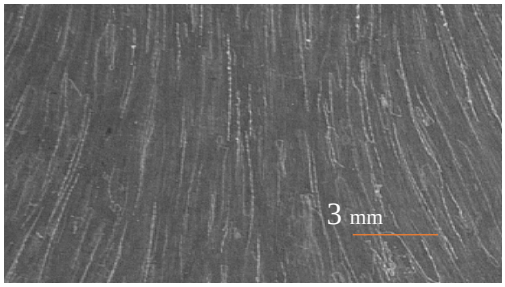

Orientation in the longitudinal direction of milling

FIG. 5 ─ Orientation of the fibers, visualized with a Leica microscope DMRX.

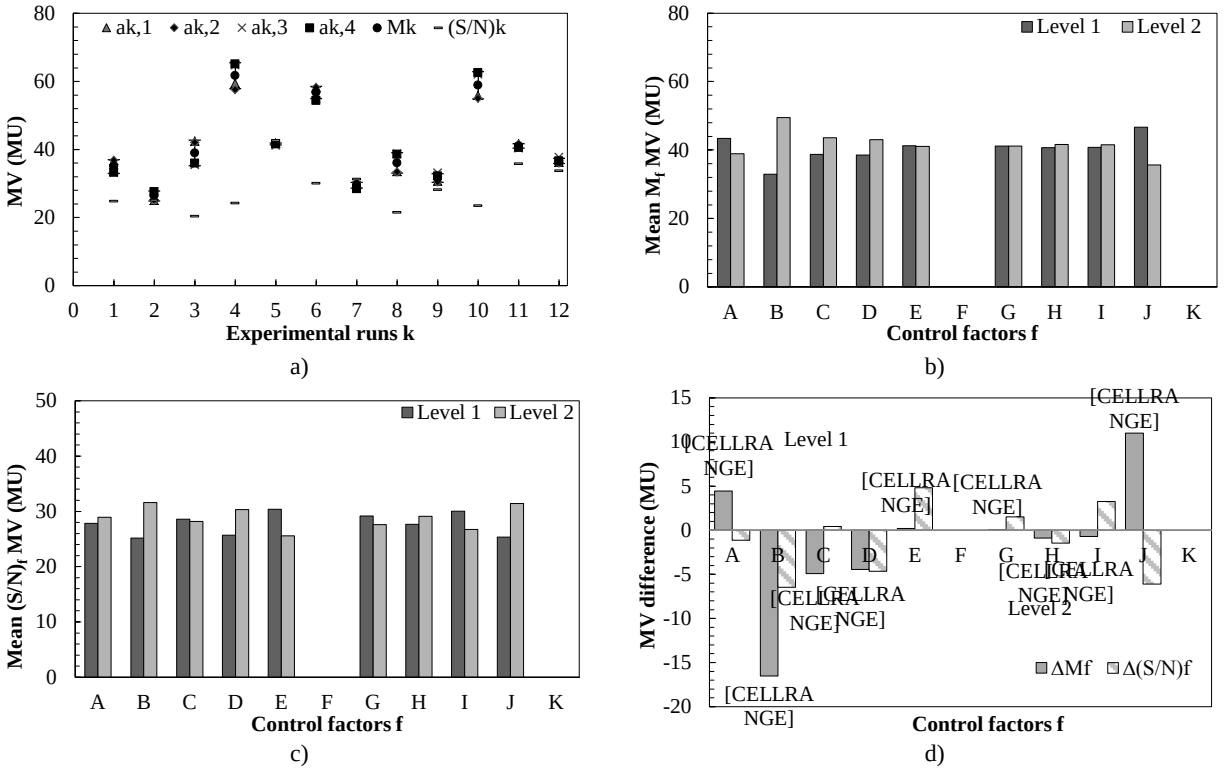

FIG. 6 ─ a) Raw data replicate plot of Mooney viscosity (MU), b) Mean Mooney viscosity per level per factor, c) S/N ratio's *MV* per level per factor and d) Difference coefficients for MV (MU) per factor.

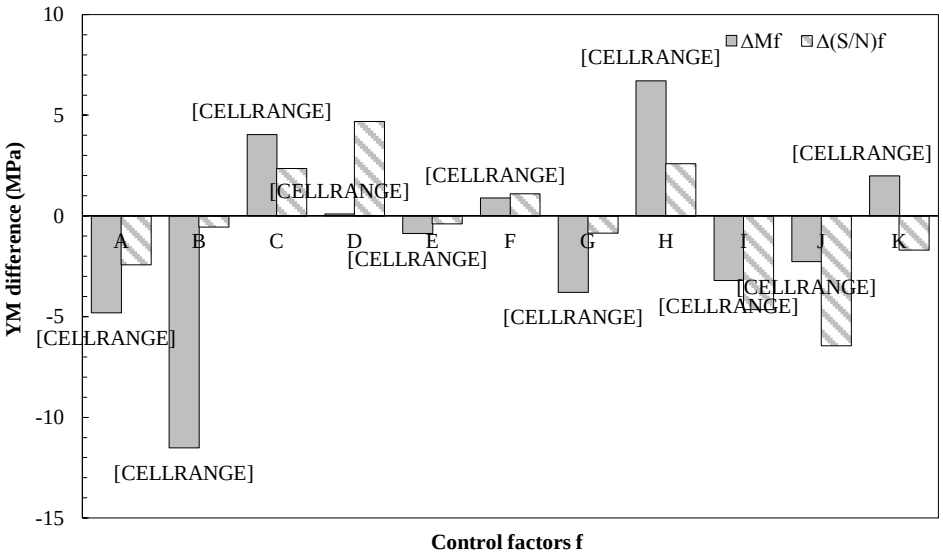

FIG. 7─ Conceptual way of graphing the Difference coefficients for Young's modulus (MPa) per control factor for DoE1.

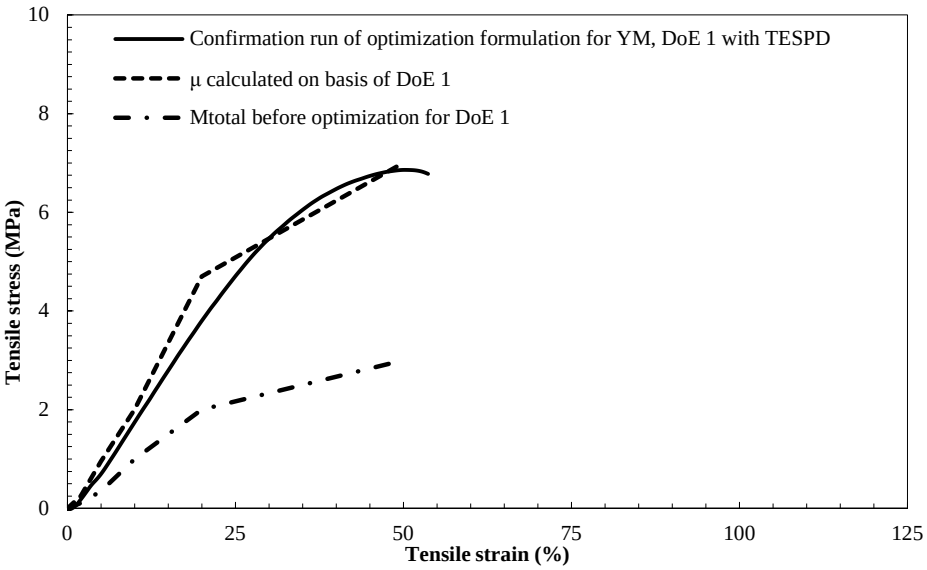

FIG. 8 ─ Tensile curve optimized for *YM* vs. M_{total} values for DoE1.

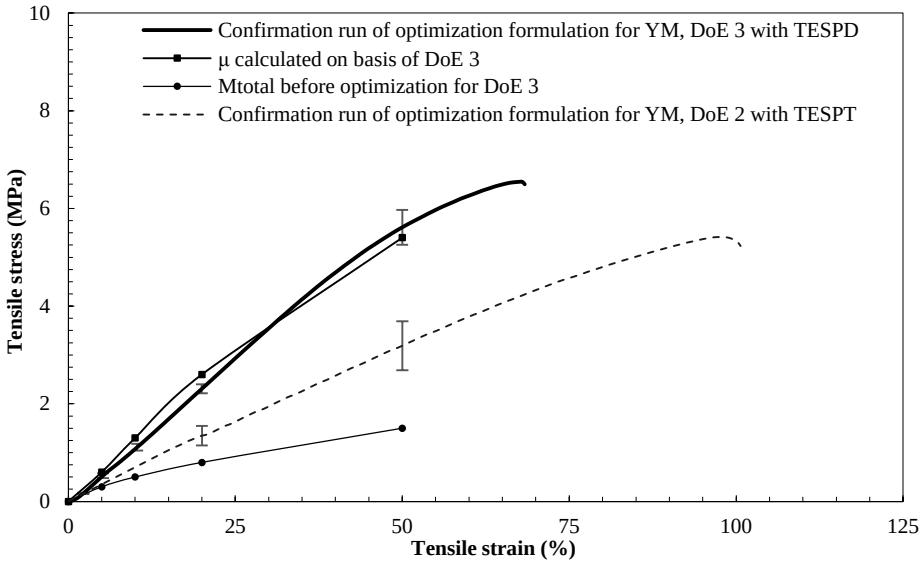

FIG. 9 ─ Tensile curve optimized for *YM* vs. M_{total} values for DoE's 2 and 3.